MECHANICAL PROPERTIES AND MICROSTRUCTURAL BEHAVIOR OF HYDROXYAPATITE/TIO2 ELECTROSPUN NANOFIBERS CONSOLIDATED USING HIGH FREQUENCY INDUCTION HEAT SINTERING

Khalil Abdel-razek Khalil

Materials Engineering and Design Department, High Institute of Energy, South Valley University, Aswan, Egypt   e-mail:Khalil305@hotmail.com

In order to improve fracture toughness of hydroxyapatite (HAp), TiO_2 electrospun nanofibers were used as reinforcement. TiO_2 nanofibers with diameters of 50–400 nm were first prepared by calcining and presintering of electrospun nanofibers of polyvinyl acetate (PVac)/Titania composite at different temperatures. The composite of HAp with 5 wt % of electrospun TiO_2 nanofibers were then sintered by high frequency induction heat sintering technique. Mechanical properties were evaluated by three-point bending tests, indentation tests and compression test. The results indicated that the morphology and crystalline phase of TiO_2 nanofibers were strongly influenced by the calcination temperature. Additionally, the SEM results showed that the nanofibers calcined at 600 °C are porous structure due to the low densification. There was a significant change of microstructure with increasing calcination temperature to 800 °C. The nanofibers were appeared with dense microstructure due to the high temperature calcination. A number of large size particles or particle aggregates connected by a small neck were found after the nanofibers were calcined at 1000 °C. The sintering behaviors, toughness and hardness of the resulting composites were significantly affected by the calcinations temperature of the included TiO_2 nanofibers. The bending and compressive strength values of HAp/5 wt. % TiO_2 composites sintered at 1050 °C were 119 and 120 MPa respectively, when the calcination temperature of the TiO_2 nanofiber was 800 °C, while the strength is decreased with decreasing or increasing calcination temperature than 800 °C.

KEYWORDS: *Hydroxyapatite, Electrospinning, nanofibers, consolidation, mechanical properties, microstructure.*

1. INTRODUCTION

Calcium hydroxyapatite (HAp, $Ca_{10} (PO_4)_6(OH)_2$) is one of the most important biocompatible materials with human bones and teeth [1]. However, the relatively low strength and susceptibility to brittle fracture of the HAp-based materials have severely limited its use to only non-load bearing application [2, 3]. Therefore, improvement in mechanical properties of HAp is necessary for load bearing application. Especially, the

improvement in fracture toughness is necessary. A suitable method of improving the mechanical properties is based on the synthesis of composites made of HAp and other second phases [4–7]. Various methods have been reported in the literature to improve the mechanical properties of HAp. For example, zirconia [8–11], glass [12–15], silver [16, 17], carbon fiber [18, 19] and HAp whiskers [20] have been used as reinforcements to improve the mechanical properties of HAp. It is well known that fibers are widely used to improve the strength and fracture toughness of brittle materials. The strengths of ceramic fibers and whiskers are of size-dependence [21]. As the diameter or gauge length decreases, the strength of ceramic fibers and whiskers increases [22–24]. Moreover, their mechanical properties such as fracture toughness and fracture strength, etc. depend on the crystal structure, compositions and sizes. Recently, electrospinning technique has been successfully employed in the preparation of some polymer and metal oxide nanofibers [25-28]. This technique has been found to be unique and cost effective approach for fabricating large surface area membranes for a variety of applications [29, 30]. Electrospun nanofibers have approximately 1 to 2 orders of magnitude more surface area than that found in thin films [31]. Khalil et. al, [32] developed HA/NiO type nano-composites using NiO electrospun nanofiber as a reinforcement with enhanced mechanical properties. Unfortunately, if the NiO fibers in the HA matrix is heated in a graphite die at high temperature in a vacuum, the fibers are very likely to have been reduced into Ni, at least partially. In this case, however, there is a serious problem. Metallic Ni is toxic and cannot be used as a biomaterial. For that TiO_2 is the best option that can be used as reinforcement in spite of NiO.

On the other hand, HA composites cannot be easily sintered without pressure [33] and the HA phase often decomposes into other phases during the conventional sintering. Furthermore, the use of conventional methods of powder consolidation often results in grain growth in the powder compact or surface contamination due to the high temperatures and long sintering duration involved. It is therefore essential to minimize grain growth through careful control of consolidation parameters, particularly temperature and sintering time. To this end, the technique of high Frequency Induction Heat Sintering (HFIHS) has been shown to be an effective sintering method which can successfully consolidate ceramics and metallic powders to near theoretical density [34-36].

This paper reports development of a production method to create a composite material that is biocompatible, which will have high mechanical strength, and be able to withstand exposure to the physiological environment.

2. EXPERIMENTAL WORK

2.1 Hydroxyapatite Powders

Hydroxyapatite (HA) powder supplied by Sigma Aldrich Corporation was used as received in this study. Figure 1 shows SEM micrographs of the hydroxyapatite powder. The HAp powders were first deagglomerated by milling in a tumbling ball mill with a ball-to-powder weight ratio of 30:1 and a powder-to-alcohol weight ratio of about 2:1. Milling was done in polyethylene bottles using zirconia balls and was performed at a horizontal rotation velocity of 250 rpm for 24 h.
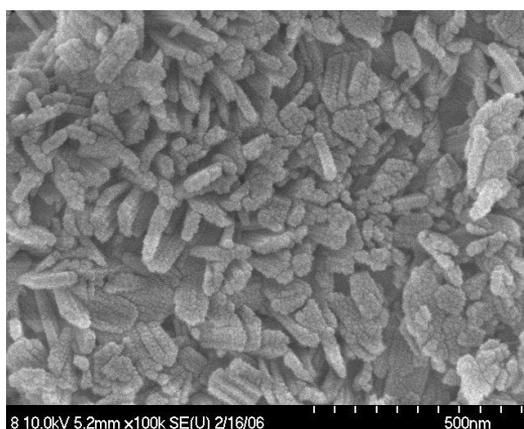
Fig. 1 SEM micrographs of the hydroxyapatite powders

2.2 Electrospinning of TiO2 nanofibers

TiO$_2$ nanofibers were prepared in the laboratory by electrospinning method as described in the literature using polyvinyl acetate (PVAc) as a template for electrospinning [8]. Polyvinyl acetate (PVAc) was obtained from Celanese Ltd. Titanium isopropoxide (TiP), N,N-dimethylformamide (DMF), and acetic acid (HAc) were purchased from Aldrich. These chemicals were used without further purification. Distilled water was used as hydrolysis agent. PVAc solution was prepared from PVAc beads and DMF with vigorous stirring. The concentration of PVAc solution tested was 11.5 wt%. A certain volume of TiP was added into the PVAc solution under vigorous stirring. Acetic acid was added to this solution under vigorous stirring to get a transparent solution. This transparent solution was placed in a plastic capillary. The plastic capillary was then clamped to a stand which was above a grounded metal mesh. The power supply was connected to the metal capillary tip. The voltage was 19 kV, and the tip-to-collector distance (TCD) was 15 cm. Nonwoven mats were collected on the surface of metal mesh. Figure 2 shows SEM micrographs of the TiO$_2$ nanofiber before calcination.
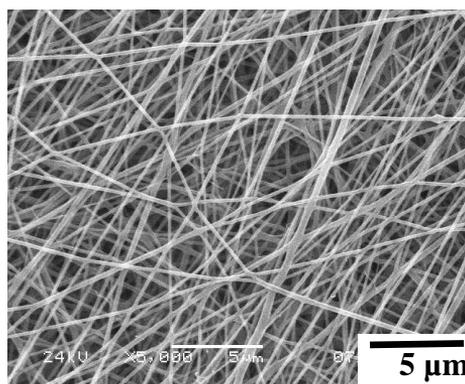

Fig. 2 SEM micrographs of the TiO$_2$ nanofiber before calcination

The nanofiber mats were then calcined at 600, 800 1000, and 1200 °C in air for 2 h to get theTiO$_2$ nanofiber aggregate. The heating rate was 10 °C min^{-1}. The morphology and diameter of the inorganic nanofibers were determined using Field Emission Scanning Electron Microscopy (FE-SEM), after gold coating with Polaron SC 7640 Sputter Coater to avoid charging. The measurement of the crystallinity was carried out at room temperature by using a Philips diffractometer with a Geiger counter, connected to a computer. The diffraction scans were collected at 2θ between 20◦ and 80◦.

2.3 Milling and Densification

Pre-sintered electrospun TiO$_2$ nanofibers with 5 wt% and calcined at different temperatures were added to the slurries and mixed with the deagglomerated HAp for 30 minuets. After mixing, the slurries were dried at 60 °C in a vacuum drying oven. The mixed composites were placed in a graphite die (outside diameter, 45 mm; inside diameter, 20 mm; height, 40 mm) and then introduced into the high-frequency induction heat sintering machine. Details of this apparatus were introduced elsewhere [32, 34-36]. The sintering process was carried out in a vacuum atmosphere at 1050 °C. The system was first evacuated to a vacuum of 28×10^{-2} torr and a 60 MPa uniaxial pressure was applied. The applied pressure was measured using a strain gage based load cell with accuracy of 0.03% to 0.25%. An induced current (frequency of about 50 kHz) was then activated and maintained until densification was observed, indicating the occurrence of the sintering and the concomitant shrinkage of the sample. Sample shrinkage was measured by a linear gauge measuring the vertical displacement. Temperatures were measured by an optical pyrometer with a range of 500 to 2000 °C and an accuracy of ± 5 °C focused on the surface of the graphite die. After sintering, the samples were ground and polished for subsequent indentation and microscopy observations. Density is determined by means of Archimedes' principle (buoyancy method), using an accurate balance with 0.1 mg accuracy. The morphologies of fracture surfaces of the composite were investigated using Field Emission Scanning Electron Microscopy (FE-SEM), after gold coating with Polaron SC 7640 Sputter Coater to avoid charging. The crystal phase of the composites before and after sintering was determined by X-ray diffraction (XRD). Vickers hardness and toughness were measured by performing indentations at a load of 500 g with holding time of 15 s. Fracture toughness is given by the values of K$_{IC}$. The factor K$_{IC}$ was determined using the direct crack measurement method [20].

3. RESULTS AND DISCUSSION

3.1 Presintering and Calcination of the TIO2 Nanofiber

Figure 3 gives FE-SEM micrographs of the TiO$_2$ nanofibers calcined at different temperatures, (a) 600 °C, (b) 800 °C and (c) 1000 °C, subscript 1 and 2 represent low and high magnifications. It can be seen that the nanofibers were burnt into rods with a rough surface because of the low content of Titania in the sol-gel solution. The surface of all calcined nanofibers was rough and the nanofibers were broken when the

calcination temperature was increased. From this observation, it is confirmed that the nanofiber calcined at 600 °C are porous structure due to the low densification Figure 3 (a). In Figure 3 (b) the low and high magnification image (b1 and b2), there were a significant change of microstructure with increasing calcination temperature to 800 ∘C. Also, there was no found porosity. In the enlarged images (b2), the nanofibers were appeared with dense microstructure due to the high calcination temperature. A number of large size particles or particle aggregates connected by a small neck were found after the nanofibers were calcined at 1000 °C (Figure 3 (c)). Meanwhile, the nanofibers have more curves on increasing the calcination temperature. The reason may be the crystalline transition and growth on increasing the calcination temperature. In a word, TiO_2 nanofiber calcined at 800 °C appeared as strong and suitable for using as reinforcement agent. All calcined samples were proved to be pure TiO_2 by means of XRD shown in Figure 4.
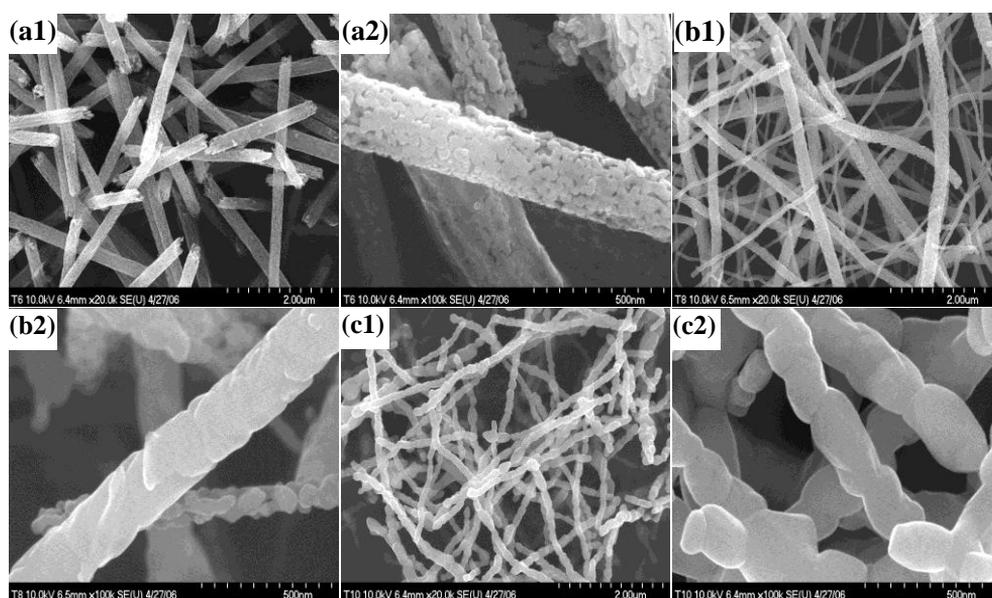
Fig. 3 FE-SEM micrographs of the TiO_2 nanofibers calcined at different temperatures, (a) 600 °C, (b) 800 °C and (c) 1000 °C (subscript 1 and 2 represent low and high magnifications.

XRD patterns of Titania nanofibers calcined at different temperature are shown in Figure 4. It can be seen that, there is no phase change for the samples of the PVac/titania nanofibers calcined at 600 °C, anatase phase were the main constituent phases in this sample. It is well known that, pure Titania crystallizes into anatase upon calcination at 400 °C [37]. When the PVac/titania nanofibers were calcined at 800 °C, a new crystalline phase around $2\theta = 26°$ appeared and this was rutile. However, when calcined at 1000 °C, complicated crystalline phase patterns in which the peaks from anatase and rutile of Titania were present. The nanofibers calcined at 1000 °C also showed the peak from anatase; however, it was sharper than that of nanofibers calcined at 600 and 800 ∘C.
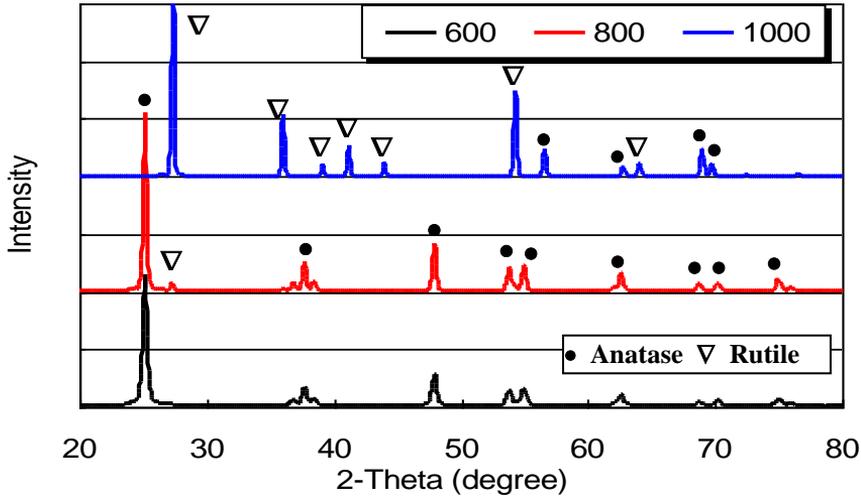
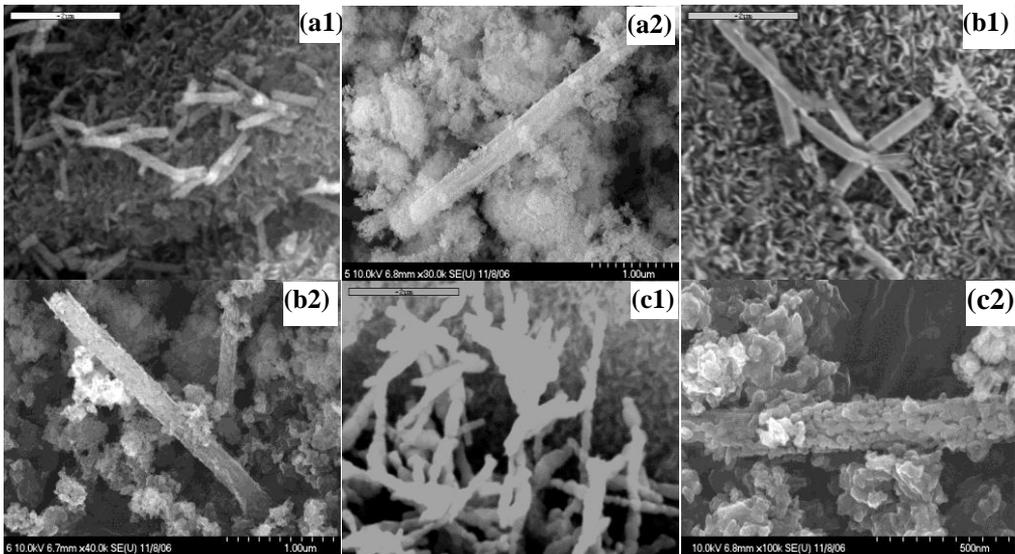Fig. 4 XRD patterns of TiO$_2$ nanofibers calcined at different temperatures.

Fig. 5 FE-SEM micrographs of the HAp/TiO$_2$ electrospun nanofiber calcined at different temperatures after deagglomeration and mixing, (a) 600 °C, (b) 800 °C and (c) 1000 °C (subscript 1 and 2 represent low and high magnifications.

　　　　Figure 5 shows morphologies of the hydroxyapatite with TiO$_2$ electrospun nanofiber after deagglomeration and mixing. From this observation, it is confirmed that the TiO$_2$ electrospun fibers were broken into small parts with aspect ratio (length to the diameter of the nanofibers) nearly 5 to 15 as shown in Figure 5 (a) to (c). In Figure 5 (a1) and (a2), the enlarged image, the nanofibers were appeared with porous structure and small aspect ratio. While in Figure 5 (b1) and (b2), the nanofiber showed with dense microstructure due to the high calcination temperature and the aspect ratio was

more high then Figure 5 (a). In Figure 5 (c1) and (c2) the nanofiber were broken into elongated particles with very low aspect ratio due to high calcination temperature at 1000 ◦C (Figure 5 (c)). Meanwhile, the nanofibers were very weak and have more curves on increasing the calcination temperature. Thus, milling results in uniform distribution of hydroxyapatite and TiO_2 electrospun nanofibers and the nanofiber was strong enough to withstand the milling force when the calcination temperature was 800 ◦C.
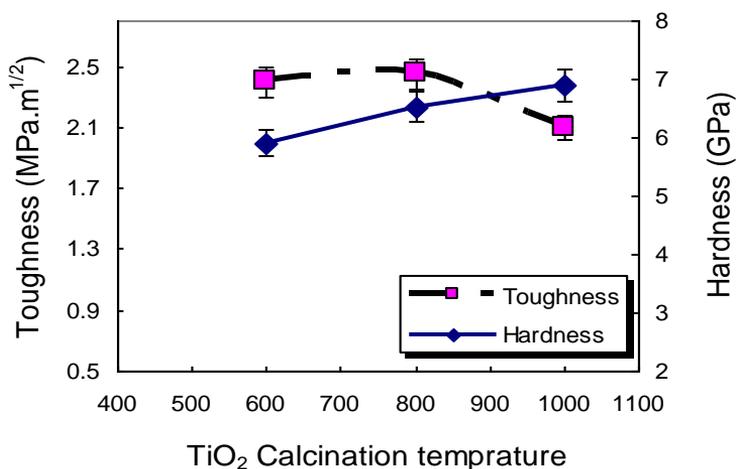

Fig 6 Hardness and toughness of HA/5%wtTiO_2 electrospun
nanofiber calcined at different temperatures.

Figure 6 shows the Vickers hardness and fracture toughness of the HA/TiO_2 electrospun nanofiber composites depending on the calcination temperatures of the electrospun nanofibers. The fracture toughness of the HA reinforced with TiO_2 nanofiber calcined at 600 °C was about 2.4 MPa. $M^{1/2}$ and slightly increased with using electrospun nanofiber calcined at 800 °C to around 2.45 MPa . $M^{1/2}$. While at 1000 ◦C calcination temperature the fracture toughness was decreased into about 2.1 MPa. $M^{1/2}$. In contrary with toughness, the Vickers hardness is slightly increased with increasing the calcination temperature of the electrospun nanofibers. The hardness of HA reinforced with TiO_2 calcined at 600 was around 5.9 GPa reached maximum (around 6.9 GPa) in the samples contains electrospun nanofiber calcined at 1000 °C, as shown in Fig. 6. Due to mixing process, the TiO_2 electrospun fibers were broken into small parts with aspect ratio (length to diameter) nearly 5 to 15. Some fragmented TiO_2 nanoparticles are also exist. However, the author suggest that, one of the reasons of the increase in the fracture toughness is attributed to the synergistic effects of crack deflection, interlocking of the fibers, pullout and crack bridging due to the fibers inclusion [38]. The other reason for the increase in fracture toughness is probably due to the presence of TiO_2 fragmented nanoparticles at the grain boundary regions. These nanosized inclusions can significantly enhance the mechanical properties of ceramics. Remarkably, with increasing calcination temperature, the TiO_2 fragmented particles increased, for that the hardness is increased. The hardness values for all of the HAp/TiO_2 electrospun nanofiber samples have narrow distribution ranges, indicating a homogeneous distribution of the toughening phase fibers in the HAp matrix. W.

Suchanek et al. [39] reported that the fracture toughness of the monolithic HAp did not exceed the value of about 1 MPa. $m^{1/2}$. However, the values of fracture toughness and Vickers hardness of HAp/TiO$_2$ electrospun nanofiber calcined at 800 ◦C were 2.45 MPa. $m^{1/2}$ and 6.91 GPa, respectively. Notably, the relative density of the HAp/TiO$_2$ electrospun nanofiber almost did not vary with the calcination temperature, being on the same level of approximately 99.5 % as shown in Fig. 7.
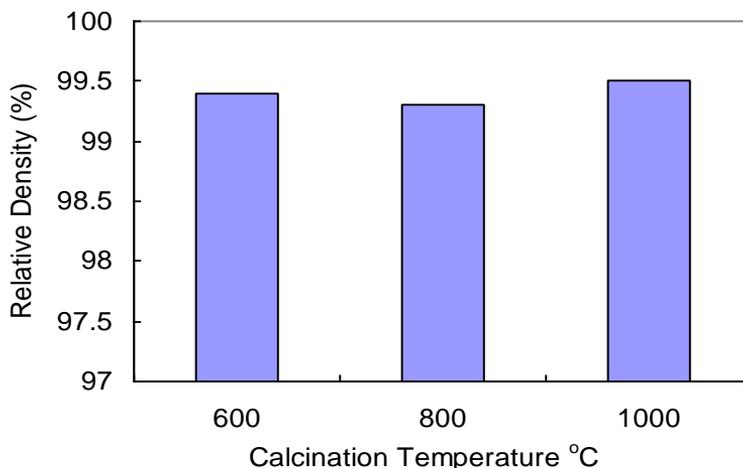

Fig 7 Relative density of HA/TiO2 electrospun nanofiber calcined at different temperatures.

Figure 8 shows the typical stress - strain curve of the HA/TiO$_2$ electrospun nanofiber composites depending on the calcination temperatures of the electrospun nanofibers. The average result of three tensile tests carried out under the same conditions for each specimen was obtained.

The dependence of ultimate tensile strength (average value for three bending test specimens) on the nanofiber calcination temperatures is given in Figure 9. It is clear that, in the sample of HA contains TiO$_2$ calcined at 600 °C, the value of bending strength was low about 90 MPa. However, as the calcination temperature of the nanofiber increased, the values of bending strength increased due to the enhancing of nanofiber density. The bending strength of the TiO$_2$ nanofiber calcined at 800 °C is reached as high as 119 MPa. Thus, when using nanofiber calcined at 1000 °C calcination temperature, the value was again decreased to about 100 MPa. Figure 10 shows the dependence of compressive strength (average value for three compression test specimens) on the nanofiber calcination temperatures. It is clear that, the samples exhibit the same behavior as bending test. In the sample of HA contains TiO$_2$ calcined at 600 °C, the value of compression strength was low about 100 MPa. However, as the calcination temperature of the nanofiber increased, the values of bending strength increased due to the enhancing of nanofiber density as mentioned before. The compressive strength of the TiO$_2$ nanofiber calcined at 800 ◦C is reached as high as 120 MPa, and the value was again decreased to about 60 MPa when using nanofiber calcined at 1000 ◦C calcination temperature.
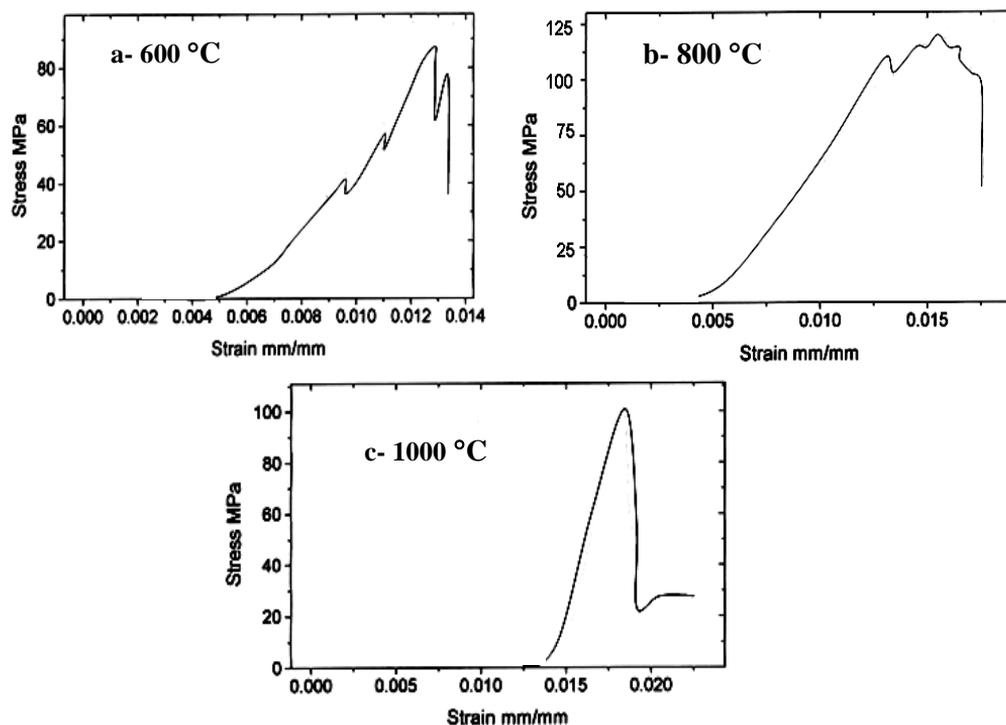
Fig. 8 Typical stress-strain curve for the composites of HA/TiO$_2$ electrospun nanofiber calcined at different temperatures. (a) 600, (b) 800 and (c) 1000 ◦C
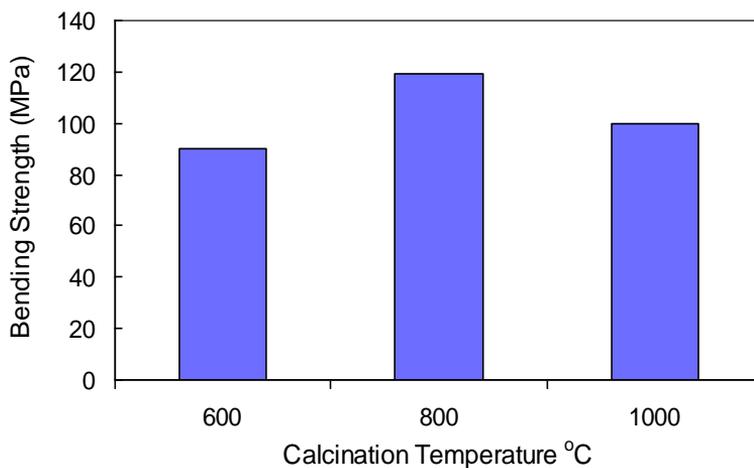

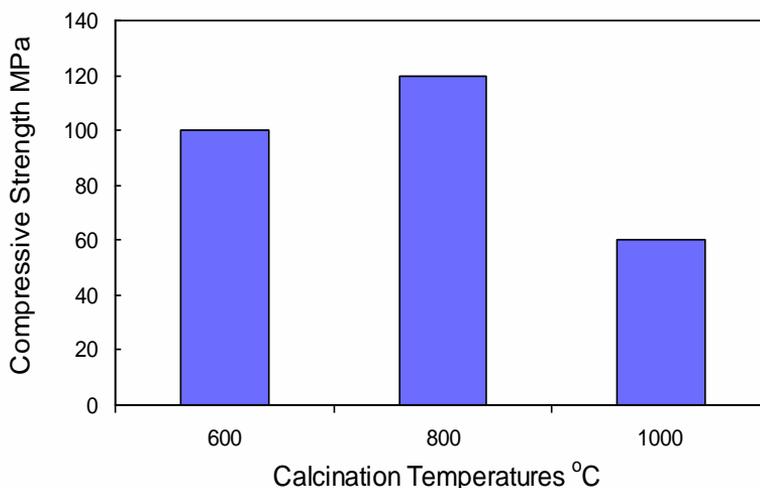Fig 9 Maximum bending strength of HA/TiO2 electrospun nanofiber calcined at different temperatures.

Fig 10 Maximum compressive strength of HA/TiO2 electrospun
nanofiber calcined at different temperatures.

SEM micrographs of the fracture surfaces of HAp containing 5wt% TiO_2 electrospun nanofibers calcined at different temperature are shown in Fig. 11 (a), (b) and (c). The addition of electrospun nanofibers led to improve the densification process and eliminate the pores [36]. As shown in Fig. 11(b) and (c), the orientation and distribution of TiO_2 nanofiber in the composites is homogeneous. The exposed fractured ends of TiO_2 nanofiber could be clearly observed. They suggest that the bonding between HAp and TiO_2 nanofiber was strong so that the TiO_2 nanofiber could easily immerse in the matrix and enhanced the toughness of HAp. It can be also observed that there are no gaps around TiO_2 nanofiber, and that the matrices of composites were dense enough under the present experimental conditions. The TiO_2 nanofibers residing at the crack front might also effectively cause crack bridging due to stresses associated with the particulate inclusions [40]. Nanofibers could be seen embedded in the fine HAp matrix. However, toughening effects due to TiO_2 electrospun nanofibers occurred only in the composites of HA contains nanofibers calcined at 800 °C. In these composites, fracture surfaces exhibited distinctive curvature, most probably owing to deflection of the propagating crack on the nanofibers. Fracture surfaces of the HA composites contains nanofibers calcined at higher temperatures were flat, because the nanofiber was broken into small parts and disappeared owing to grain growth and crack went transgranularly without any deflection.

XRD patterns of the pure HAp ceramic and the composite with 5 wt.% TiO_2 electrospun nanofiber after HFIHS pressing in the same conditions are shown in Fig. 12. Compared with these profiles, HA phase was the main constituent phase and some peaks corresponding to TiO_2 are observed in the composite sample. There is no new crystalline phase was formed during the sintering by HFIHS indicating that no chemical reactions between HA and the TiO_2. No decomposition of the HAp phase was observed as a result of the sintering process.
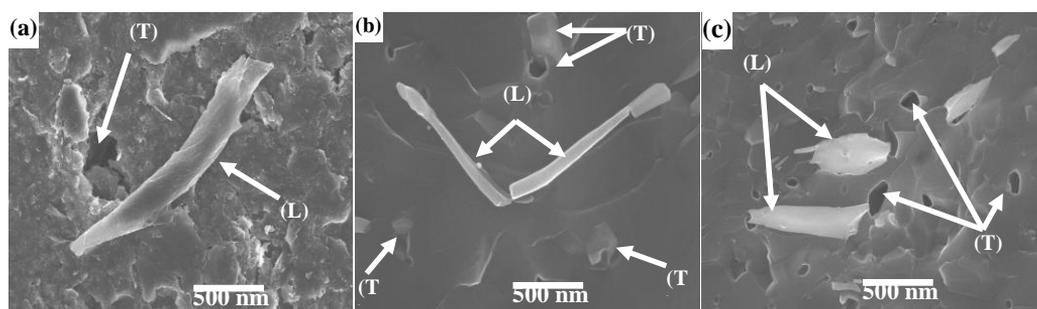
Fig. 11 FE-SEM micrographs of the fracture surface HAp / 5wt% TiO_2 calcined at different temperatures (a) 600 (b) 800 (c) 1000 ◦C. TiO_2 nanofibers are indicated by the white arrows. (L) Longitudinal direction, (T) Transverse direction
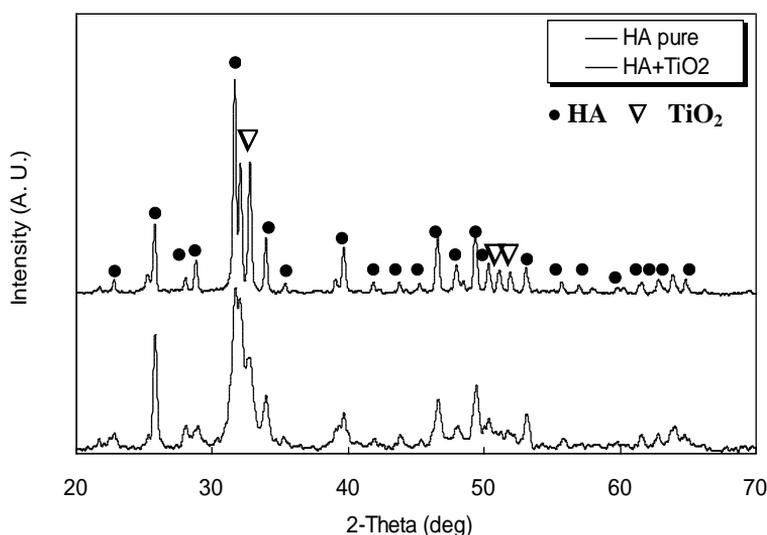

Fig. 12 XRD patterns of the pure hydroxyapatite ceramic and the composite with 5 wt. % TiO_2 electrospun nanofiber.

4. CONCLUSIONS

Titanium oxide nanofibers prepared by Electrospinning technique have been used as reinforcements of the HAp ceramics. TiO_2 nanofibers with diameters of 50–400 nm were first prepared by calcining and presintering of electrospun nanofibers of polyvinyl acetate (PVac)/Titania composite at different temperatures. Nanocomposites of HAp/TiO_2 with 5 wt % of electrospun TiO_2 nanofibers were synthesized and densified very rapidly at 1050 °C to nearly full density by High-frequency induction heat sintering (HFIHS). The results showed that:

1.   The morphology and crystalline phase of TiO_2 nanofibers were strongly influenced by the calcination temperature. The nanofibers calcined at 600 °C were porous structure due to the low densification, while with increasing

calcination temperature to 800 °C there was a significant change of microstructure. The nanofibers were appeared with dense microstructure due to the high temperature calcination. A number of large size particles or particle aggregates connected by a small neck were found after the nanofibers were calcined at 1000 °C.

2.   The sintering behaviors, toughness and hardness of the resulting composites were significantly affected by the calcinations temperature of the included TiO_2 nanofibers. The optimum mechanical properties have been achieved for composites containing electrospun nanofibers calcined at 800 °C. Density of such HA/TiO_2 composites was in the range of 99 -99.5 % of the theoretical density. The bending and compressive strength values were 119 and 120 MPa respectively at 800 °C. Vickers hardness was in the range of 6 – 7 GPa. Fracture toughness of the composites reflected their microstructure and was around the value of 2.45 MPa. $m^{1/2}$

ACKNOWLEDGEMENTS

REFERENCES

1.   R.Z. LeGeros, J.P. LeGeros, in: L.L. Hench, J. Wilson (Eds.), An Introduction to Bioceramics, World Scientific Publishing, Singapore, 1993, p. 139.

2.   A.J. Ruys, M. Wei, C.C. Sorrell, M.R. Dickson, A. Brandwood, B.K. Milthorpe, Sintering effect on the strength of hydroxyapatite, Biomaterials 16 (1995) 409–415.

3.   G. Muralithran, S. Ramesh, The effects of sintering temperature on the properties of hydroxyapatite, Ceram. Int. 26 (2000) 221–230.

4.   J. Li, B. Fartash, L. Hermansson, Hydroxyapatite-alumina composites and bone-bonding, Biomaterials 16 417–422, 1995

5.   V.V. Silva, F.S. Lameiras, R.Z. Dominggues, Synthesis and characterization of calcia partially stabilized zirconia-hydroxyapatite powders prepared by co-precipitation method, Ceram. Int. 27 615–620, 2001

6.   X. Miao, A.J. Ruys, B.K. Milthorpe, Hydroxyapatite-316L fibre composites prepared by vibration assisted slip casting, J. Mater. Sci. 36 (13) 3323–3332, 2001

7.   K. Kato, Y. Eika, Y. Ikada, In situ hydroxyapatite crystallization for the formation of hydroxyapatite/polymer composites, J. Mater. Sci. 32 (20) 5533–5543, 1997

8.   Li J, Liao H, Hermansson L. Sintering of partially-stabilized zirconia and partially-stabilized zirconia-hydroxyapatite composites by hot isostatic pressing and pressureless sintering. Biomaterials, 1996; 17:1787–90.

9. Delgado JA, Morejo´n L, Martı´nez S, Ginebra MP, Carlsson N, Ferna´ndez E, et al. Zirconia-toughened hydroxyapatite ceramic obtained by wet sintering. J Mater Sci Mater Med 1999; 10:715–9.

10. Shen Z, Adolfsson E, Nygren M, Gao L, Kawaoka H, Niihara K. Dense hydroxyapatite-zirconia ceramic composites with high strength for biological applications. Adv Mater 2001; 13:214–6.

11. Towler MR, Gibson IR. The effect of low levels of zirconia addition on the mechanical properties of hydroxyapatite. J Mater Sci Lett 2001; 20:1719–22.

12. Knowles JC, Bonfield W. Development of a glass reinforced hydroxyapatite with enhanced mechanical properties. The effect of glass composition on mechanical properties and its relationship to phase change. J Biomed Mater Res 1993; 27:1591–8.

13. Santos JD, Knowles JC, Reis RL, Monterio FJ, Hastings GW. Microstructural characterization of glass-reinforced hydroxyapatite composites. Biomaterials 1994;15:5–10.

14. Lopes MA, Monterio FJ, Santos JD. Glass-reinforced hydroxyapatite composites: fracture toughness and hardness dependence on microstructural characteristics. Biomaterials 1999; 20:2085–90.

15. Oktar FN, Go¨ ller G. Sintering affects on mechanical properties of glass-reinforced hydroxyapatite composites. Ceram Int 2002; 28:617–21.

16. Chaki TK, Wang PE. Densification and strengthening of silver reinforced hydroxyapatite-matrix composite prepared by sintering. J Mater Sci Mater Med 1994; 5:533–42.

17. Zhang X, Gubbels GHM, Terpstra RA, Metselaar R. Toughening of calcium hydroxyapatite with silver particles. J Mater Sci 1997; 32:235–43.

18. S´ lo´sarczyk A, Klisch M, Bła_zewicz M, Piekarczyk J, Stobierski L, Rapacz-Kmita A. Hot pressed hydroxyapatite-carbon fibre composites. J Eur Ceram Soc 2000;20:1397–402.

19. Park K, Vasilos T. Characteristics of carbon fibre-reinforced calcium phosphate composites fabricated by hot pressing. J Mater Sci Lett 1997;16:985–7.

20. Suchanek W, Yashima M, Kakihana M, Yoshimura M. Hydroxyapatite/ hydroxyapatite-whisker composites without sintering additives: mechanical properties and microstructural evolution. J Am Ceram Soc 1997; 80:2805–13.

21. S.C. Bennett, D.J. Johnson, J. Mater. Sci. 18 (1983) 3337.

22. A. Kelly, Strong Solids, Clarendon Press, Oxford, UK, 1973, p. 254.

23. S.B. Batdorf, in: A. Kelly (Ed.), Strength of Composites (Statistical Theory): Concise Encyclopedia of Materials, Revised Edition, Elsevier, Oxford, UK, 1994.

24. K.B. Prewo, J. Mater. Sci. 21 (1986) 3590.

25. D.H. Reneker, A.I. Yarin, H. Fong, S. Kombonge, J. Appl. Phys. 87 (2000) 4531.

26. J. Doshi, D.H. Reneker, J. Electrostst. 35 (1995) 151.

27. N. Dharmaraj , H.C. Park , B.M. Lee , P.Viswanathamurthi , H.Y. Kim, D. R. Lee, Inorg. Chem. Commun., 7 (2004) 431.

28. N. Dharmaraj , H.C. Park , C.K. Kim , H.Y. Kim, D. R. Lee, Mater. Chem. Phys. 87 (2004) 5.

29. K.H. Lee, H.Y. Kim, M.S. Khil, Y.M. La, D.R. Lee, polymer 44 (2003) 1287.
30. D.H. Reneker, A.L. Yarin, H. Fong, S. Kombonge, J. Appl. Phys. 87 (2000) 4531.
31. P. Gibson, H. Schreuder-Gibson, D. Riven, Colloids Surf. A 187 (2001) 46
32. Khalil Abdelrazek Khalil and Sug Won Kim, Effect of Processing Parameters on the Mechanical and Microstructural Behavior of Ultra-Fine Al_2O_3–(ZrO_2-8%Mol Y_2O_3) Bioceramic, Densified By High-Frequency Induction Heat Sintering, Int. J. Appl. Ceram. Technol., 3 [4] 322–330 (2006)
33. J. Li, H. Liao, L. Hermanson, Sintering of partially-stabilized zirconia and partially-stabilized zirconia—hydroxyapatite composites by hot isostatic pressing and pressureless sintering, Biomaterials Vol. 17, No. 18, pp. 1787-1790, 1996
34. H. Ch. Kim , Dong Young Oh , Synthesis of WC and dense WC-5Vol.%Co hard materials by high- frequency induction heated combustion, Materials Science and Engineering A, Vol. 368, pp 10 – 17, (2004)
35. Sug Won Kim and Khalil Abdel-Razek Khalil High-Frequency Induction Heat Sintering of Mechanically Alloyed Alumina–Yttria-Stabilized Zirconia Nano-Bioceramics, J. Am. Ceram. Soc., 89 [4] 1280–1285 (2006)
36. Khalil Abdelrazek Khalil and Hak Yong Kim, Observation of Toughness Improvement of the Hydroxyapatite Bioceramics Densified Using High-Frequency Induction Heat Sintering, Int. J. Appl. Ceram. Technol., 4 [1] 30–37 (2007).
37. [27] Khalil K M S and Zaki M I 1997 *Powder Technol.* 92 233
38. Y. Zhang, S. Tan, Y. Yin, C-fibre reinforced hydroxyapatite bioceramics, Ceramics International, Vol. 29, No. 1, pp. 113–116, 2003.
39. Suchanek,W.,Yashima, M., Kakihana, M. and Yashima, M., Hydroxyapatite ceramics with selected sintering additives. *Biomaterials*, 1997, 18, 923–933.
40. Jiao S, Jenkins ML, Davidge RW, Processing and fracture toughness of nano sized Cu dispersed Al_2O_3 composites, Acta Metall, Vol. 45, pp. 149–156, 1997

الخواص الميكانيكية والسلوك المايكروسكوبى لمركب ملبد من مسحوق الهايدروكسى اباتايت الناعم لحجم النانو والمدعم بالياف بالغة الصغر من مادة ثاني أكسيد التيتانيوم .

في هذا البحث تم استخدام الياف بالغة الصغر فى حجم النانوميتر من مادة ثانى اكسيد التيتانيوم ومصنعة بطريقة الغزل بالشحنه الكهربية لتقوية المنتجات المصنعة من مادة الهايدروكسى اباتايت التى تتوافق بايولوجيا مع مكونات عظام واسنان الانسان. فى البداية تم تصنيع وتجهيز الياف من مركب التيتانيوم ايزبروبوكسايد والبولى فينيل اسيتات باقطار تتراوح من 50 الى 400 نانوميتر . ثم بعد ذلك تم وضع هذه الالياف فى افران لاستخلاص مادة البولى فينيل اسيتات وتحويل الياف التيتانيوم ايزبروبوكسايد الى الياف ثانى اكسيد التيتانيوم وتسمى هذه العملية عملية الكلسنة والتلبيد الاولى. فى هذا

البحث تم دراسة تاثير درجة حرارة الكلسنة والتلبيد الاولى على الطور البلورى والبنية المايكروسكوبية للالياف المصنعة بغرض انتاج الياف قوية يمكن استخدامها كمقويات لمادة الهايدروكسى اباتايت. تم استخدام ثلاثة درجات حرارة مختلفة لكلسنة وتلبيد الالياف وانتاج ثلاث انواع من الالياف بحسب درجة الحرارة التى استخدمت فى الكلسنة والتلبيد الاولى. ثم تم خلط الثلاث انواع المختلفة من الالياف مع مادة الهايدروكسى اباتايت بنسبة 5% نسبة وزنية وتلبيدها بطريقة الحرارة الناتجة عن تيار الحث الذاتى عالى التردد. تم دراسة تاثير درجة حرارة الكلسنة والتلبيد الاولى للالياف المستخدمة كمقويات على الخواص الميكانيكية والبنية المايكروسكوبية للمركب النهائى. ولقد خلص البحث الى النتائج التالية: لقد وجد ان البنية المايكروسكوبية والطور البلورى لالياف اكسيد التيتانيوم قد تاثرت تاثيرا كبيرا بتغيير درجة حرارة الكلسنة والتلبيد الاولى. وفى هذا الاطار وجد ان الالياف التى تم كلسنتها عند درجة حرارة 600 درجة مئوية تتميز ببنية مسامية وكثافة منخفضة. مع زيادة درجة حرارة الكلسنة الى 800 درجة مئوية وجد ان البنية المايكروسكوبية قد تغيرت تغييرا ملحوظا، حيث اختفت المسامية وظهر جليا ان الالياف قد ظهرت بكثافة عالية. مع زيادة درجة الحرارة الى 1000 درجة مئوية وجد ان الالياف قد تحولت الى تجمعات من الحبيبات الكبيرة الحجم نوعيا والمتصلة فيما بينها عن طريق عنق صغير. وجد ايضا ان كفاءة التصليد والخواص الميكانيكية قد تاثرت تاثيرا كبيرا باختلاف درجة حرارة الكلسنة والتلبيد الاولى للالياف المستخدمة كمقوى. اخيرا يمكن القول ان الالياف التى تم كلسنتها وتلبيدها اوليا عند درجة حرارة 800 درجة مئوية كانت افضل نسبيا من حيث استخدامه كمقوى لمادة الهيدروكسى اباتايت.